

First Observation of the $\beta 3\alpha p$ Decay of ^{13}O via β -Delayed Charged-Particle Spectroscopy

J. Bishop^{1,*}, G. V. Rogachev^{1,2,3}, S. Ahn⁴, M. Barbui¹, S. M. Cha⁴, E. Harris^{1,2}, C. Hunt^{1,2}, C. H. Kim⁵,
D. Kim⁴, S. H. Kim⁶, E. Koshchiy¹, Z. Luo^{1,2}, C. Park⁴, C. E. Parker¹, E. C. Pollacco⁷, B. T. Roeder¹,
M. Roosa^{1,2}, A. Saastamoinen¹, and D. P. Scriven^{1,2}

¹Cyclotron Institute, Texas A&M University, College Station, Texas 77843, USA

²Department of Physics and Astronomy, Texas A&M University, College Station, Texas 77843, USA

³Nuclear Solutions Institute, Texas A&M University, College Station, Texas 77843, USA

⁴Center for Exotic Nuclear Studies, Institute for Basic Science, 34126 Daejeon, Republic of Korea

⁵Department of Physics, Sungkyunkwan University (SKKU), Seoul 16419, Republic of Korea

⁶Department of Physics, Sungkyunkwan University, Suwon 16419, Republic of Korea

⁷IRFU, CEA, Université Paris-Saclay, Gif-Sur-Yvette 91190, France

 (Received 27 February 2023; revised 25 April 2023; accepted 11 May 2023; published 2 June 2023)

The β -delayed proton decay of ^{13}O has previously been studied, but the direct observation of β -delayed $3\alpha p$ decay has not been reported. Rare $3\alpha p$ events from the decay of excited states in $^{13}\text{N}^*$ provide a sensitive probe of cluster configurations in ^{13}N . To measure the low-energy products following β -delayed $3\alpha p$ decay, the Texas Active Target (TexAT) time projection chamber was employed using the one-at-a-time β -delayed charged-particle spectroscopy technique at the Cyclotron Institute, Texas A&M University. A total of 1.9×10^5 ^{13}O implantations were made inside the TexAT time projection chamber. A total of 149 $3\alpha p$ events were observed, yielding a β -delayed $3\alpha p$ branching ratio of 0.078(6)%. Four previously unknown α -decaying excited states were observed in ^{13}N at 11.3, 12.4, 13.1, and 13.7 MeV decaying via the $3\alpha + p$ channel.

DOI: 10.1103/PhysRevLett.130.222501

Introduction.—Exotic neutron-deficient nuclei provide an excellent opportunity to explore new decay modes. Large β -decay Q values make it possible to populate proton- or α -unbound states in daughter nuclei, paving the way for observation of β -delayed charged-particle emissions. Reviews of advances in β -delayed charged-particle emission studies can be found in Refs. [1,2], where β -delayed one-, two-, and three-proton decays as well as $\alpha p/p\alpha$ decays are discussed. Here, we report on a new decay mode that has not been observed before, the $\beta 3\alpha p$. Not only do we identify these exotic decays of ^{13}O , but we were also able to use it to obtain information on cluster structure in excited states of the daughter nucleus, ^{13}N .

Clustering phenomena are prevalent in light nuclei and are an excellent testing ground for understanding few-body systems that are theoretically accessible. These clustering phenomena have been well studied in α -conjugate nuclei. Much less experimental information is available for $N \neq Z$ nuclei. Yet, theoretical studies (e.g., Refs. [3–5]) indicate that cluster configurations may be even richer in non-self-conjugate nuclei, opening a window of opportunity to confront the highly nontrivial theoretical predictions with experimental data. Recent experimental studies of clustering in non-self-conjugate nuclei already produced exciting results, such as hints for linear chain structures stabilized by “extra” nucleons (e.g., Refs. [6–8]) and indications for superradiance [9,10].

Of particular interest is the nucleus ^{13}N , where three α particles and an “extra” proton can form exotic cluster configurations. Resonant $^9\text{B} + \alpha$ scattering or α -transfer reactions are not possible, because ^9B is proton unbound with a half-life of the order of 10^{-18} s. Instead, one may use β -delayed charged-particle spectroscopy to populate states in ^{13}N via ^{13}O and observe the decays to a final state of $3\alpha p$. The β -delayed proton channel has previously been studied for ^{13}O [11], where limited statistics showed only a very small sensitivity to populating the $p + ^{12}\text{C}(0_2^+)$ (Hoyle state) which results in a $3\alpha + p$ final state. Utilizing the Texas Active Target (TexAT) time projection chamber (TPC) to perform one-at-a-time β -delayed charged-particle spectroscopy, α decays from the near α -threshold excited states in ^{13}N have been observed for the first time, providing insights into the $\alpha + ^9\text{B}$ clustering. Capitalizing on the advantages of TPCs for β -delayed charged-particle emission studies, unambiguous and background-free identifications of the $\beta 3\alpha p$ events were made. Reconstruction of complete kinematics for these exotic decays allowed for robust decay channel assignments, providing insights into the cluster structure of the ^{13}N excited states. Evidence for the $\frac{1}{2}^+$ first excited state in ^9B , mirror of the well-known $\frac{1}{2}^+$ in ^9Be , was an unexpected by-product of these measurements, demonstrating the sensitivity of the technique.

Experimental setup.—The β -delayed charged-particle spectroscopy technique with the TexAT TPC has previously been applied for β -delayed 3α decay studies of ^{12}N via $^{12}\text{C}^*$ [12]. A detailed description of the technique is provided in Ref. [13]. Here, we utilize the same experimental approach to observe the β -delayed $3\alpha p$ decays of ^{13}O via $^{13}\text{N}^*$. We implant β -decaying ^{13}O ($t_{1/2} = 8.58$ ms) one at a time into the TexAT TPC by providing a phase shift signal to the K500 Cyclotron at Texas A&M University when a successful implantation has taken place to halt the primary beam. This phase shift then lasts for three half-lives or until the observation of a β -delayed charged particle in TexAT, with the data acquisition ready to accept the trigger. The phase shift is then reset to allow for the next implantation. A beam of ^{13}O was produced via the $^3\text{He}(^{14}\text{N}, ^{13}\text{O})$ reaction at the momentum achromat recoil separator [14] with a typical intensity of 5 pps with an energy of 15.1 MeV/ u , degraded by an aluminum foil to 2 MeV/ u , to stop inside of the TexAT sensitive area, filled with 50 Torr of CO_2 gas. To measure the correlated implantation and decay events, the $2p$ trigger mode of general electronics system for TPCs (GET) electronics [15] was employed where the occurrence of two triggers within a 30 ms time window was required for a full event. The first trigger, the $L1A$ (implantation), is generated if the Micromegas pad multiplicity exceeds 10. If, during the 30 ms following the $L1A$ trigger, another trigger occurs with Micromegas pad multiplicity above two, the second $L1B$ (decay) trigger event and the time between the $L1A$ and $L1B$ are recorded. For normalization and beam characterization, all events were recorded, even if the $L1B$ trigger never came.

Analysis.—The complete $L1A(\text{implant}) + L1B(\text{decay})$ events were selected with the time between the two triggers in the range of 1–30 ms. The short times (< 1 ms) were omitted to remove double trigger events due to sudden beam-induced noise. To ensure the implanted ion is ^{13}O , the energy deposited by the beam implant event in the Micromegas “Jr” (MM Jr) beam tracker [16] at the entrance to the TexAT chamber was recorded. The beam contaminants were ^7Be and ^{10}C , dominated by ^7Be at $\approx 28\%$ of the beam intensity.

Following an identification of ^{13}O implant, the stopping position was evaluated event by event using implant tracks, selecting only those which stopped inside the active area of the Micromegas and not closer than 31.5 mm from the edge. The spread of the ^{13}O stopping position inside TexAT was 67.5 mm due to straggling.

Further selection was performed by imposing tight correlation (< 5 mm) between the ^{13}O stopping location and the vertex location of the respective decay event. Events which passed this test were then fit with a single track segment using a randomly sampled χ -squared minimization algorithm. If a good fit is achieved, these events were identified as single proton events. The β -delayed proton spectrum replicates the previous results [11] well,

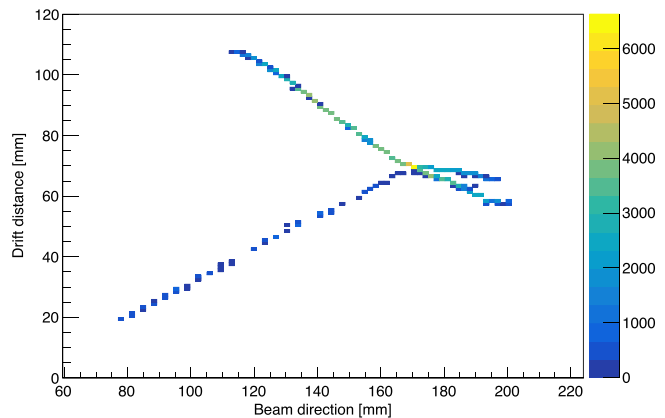


FIG. 1. Example $3\alpha + p$ event where the color (online) corresponds to the energy deposition within each voxel after projection into 2D. The proton tracks extends from the vertex to the lower-left of the figure as evidenced by the lower energy deposition. Invariant mass reconstruction designated this event as decaying through the $^9\text{B}(\text{g.s.}) + \alpha$ channel.

albeit with decreased resolution that will be covered in a subsequent publication with further experimental details. The remaining events were fit with four track segments as candidates for $\beta 3\alpha p$ decay using randomly sampled χ -squared minimization. They were then inspected visually to evaluate the fits’ quality. Given the complexity of the fits, manual modifications of the fit algorithm parameters were required for some events.

3 α + proton events.—Overall, 149 $\beta 3\alpha p$ events were identified, an example of which is shown in Fig. 1. Because of the size of the TPC and limitations on reconstruction in parts of the TexAT TPC, only 102 out of 149 of these events allow for complete reconstruction. The “incomplete” events are dominated by the $^9\text{B}(\text{g.s.}) + \alpha$ decay, as this produces a high-energy α particle that may escape from the active volume of the TexAT TPC. The efficiency for the α_0 decay starts to deviate from 100% at $E_x = 10$ MeV, slowly drops to around 60% at $E_x = 14$ MeV (where α_i signifies $\alpha + ^9\text{B}$ decay with ^9B in the i th excited state). The efficiency for α_1 and α_3 is less affected and decreases only to 70% at $E_x = 14$ MeV. In proton decays to the Hoyle state, most of the energy is taken by protons, and the resulting three α tracks of the preselected events are always confined to the active volume of the TPC. Proton tracks were not required in reconstruction, as complete kinematics can be recovered from the remaining three α tracks. Therefore, there was no efficiency reduction for the $p + ^{12}\text{C}(\text{Hoyle})$ decays.

In order to identify the parent state in $^{13}\text{N}^*$, the lowest-energy deposition arm was identified as the proton track, and the momentum of the three α particles was determined by the length and direction of α tracks in the gas. Protons almost always escape the sensitive volume, and the proton momentum is reconstructed from momentum conservation. The decay energy is then the sum of the three α particles’ and proton energy. From here, the ^8Be (Fig. 2), ^9B (Fig. 3),

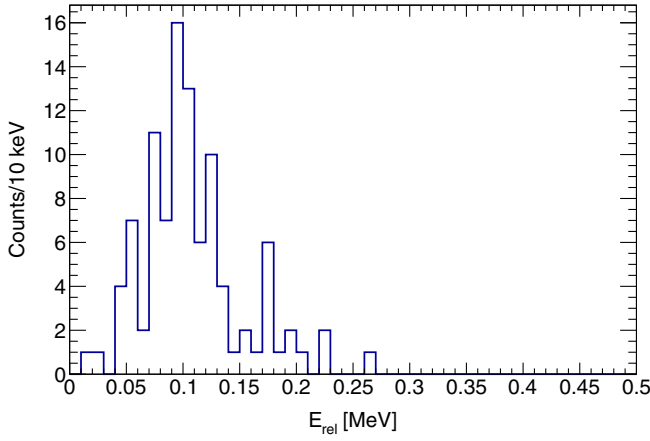


FIG. 2. Relative energy spectrum for pairs of α particles with the smallest relative energy of the three α tracks. The ${}^9\text{Be}(\text{g.s.})$ at 92 keV is well reproduced.

and ${}^{12}\text{C}$ (Fig. 4) excitation energies were determined from the invariant mass. This allowed for a selection of events which proceeded to decay via $p + {}^{12}\text{C}(0_2^+)$ [p_2], $\alpha + {}^9\text{B}(\text{g.s.})$ [α_0], $\alpha + {}^9\text{B}(\frac{1}{2}^+)$ [α_1], and $\alpha + {}^9\text{B}(\frac{5}{2}^+)$ [α_3]. There is evidence of strength in ${}^9\text{B}$ between 1 and 2.4 MeV excitation energy (Fig. 3). It is likely due to the $\frac{1}{2}^+$ state in ${}^9\text{B}$ [17] that is the mirror of the well-known $\frac{1}{2}^+$ first excited state in ${}^9\text{Be}$. Attempts to fit the spectrum without the $\frac{1}{2}^+$ in ${}^9\text{B}$ fail, because it is difficult to explain the excess of counts at excitation energies between 1.4 and 2.4 MeV comparable to the 2.4–3.5 MeV region where

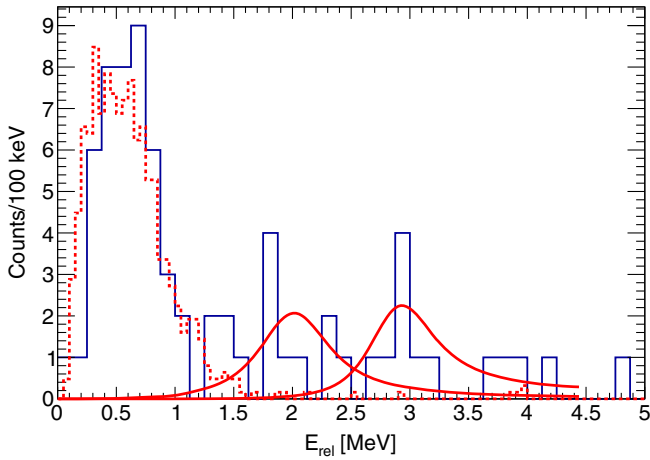


FIG. 3. For events that do not decay via the Hoyle state, the relative energy spectrum is shown here which is generated by selecting the two α particles that produce the ${}^9\text{Be}(\text{g.s.})$ and then reconstructing the ${}^9\text{B}$ relative energy with the proton. Overlaid in dashed red are simulated data for the ground state contribution and in solid red are the $\frac{1}{2}^+$ and $\frac{5}{2}^+$ states from single channel R -matrix calculations convoluted with a Gaussian with $\sigma = 0.23$ MeV. The $\frac{1}{2}^+$ parameters are those obtained by Wheldon *et al.* [17], which show excellent agreement.

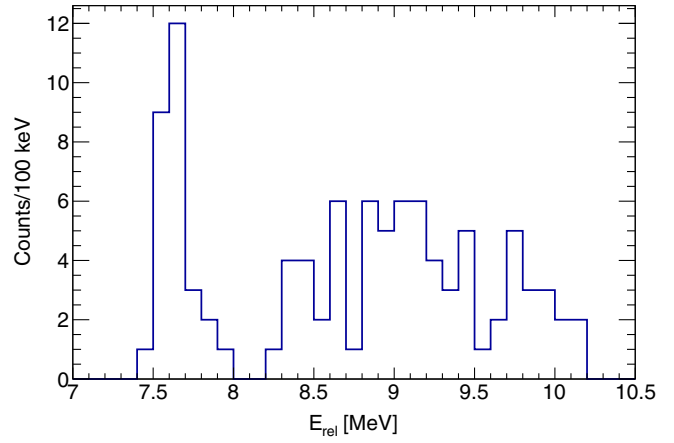


FIG. 4. Invariant mass spectrum from 3α particles assuming a ${}^{12}\text{C}$ origin. A peak at 7.65 MeV is seen, well reproducing the Hoyle state energy, and a broad peak is seen at higher excitation energies which correspond to events that decay via ${}^9\text{B} + \alpha$. No peaks from higher excited states in ${}^{12}\text{C}$ can be seen.

there are known excited state in ${}^9\text{B}$ states. Contributions from a broad $\frac{1}{2}^-$ state at 2.78 MeV may give a signature similar to that seen albeit at lower energies [peaking at $E_{\text{rel}} = 1.3$ MeV for a ${}^{13}\text{N}(E_x) = 12.4$ MeV] when considering the expected yield from a $\frac{1}{2}^-$ state in ${}^{13}\text{N}$. The $L = 0$ α decay to the broad $\frac{1}{2}^-$ in ${}^9\text{B}$ will increase the yield at small excitation energies. While this possibility is disfavored from the observed spectrum due to the energy offset, it is mentioned here for completeness. The $\frac{1}{2}^+$ state in ${}^9\text{B}$ was selected by taking an excitation energy of between 1.4 and 2.4 MeV in ${}^9\text{B}$ [following the centroid and width as observed via ${}^9\text{Be}({}^3\text{He}, t)$ [17], which is consistent with our current results], and the $\frac{5}{2}^+$ was taken as having an

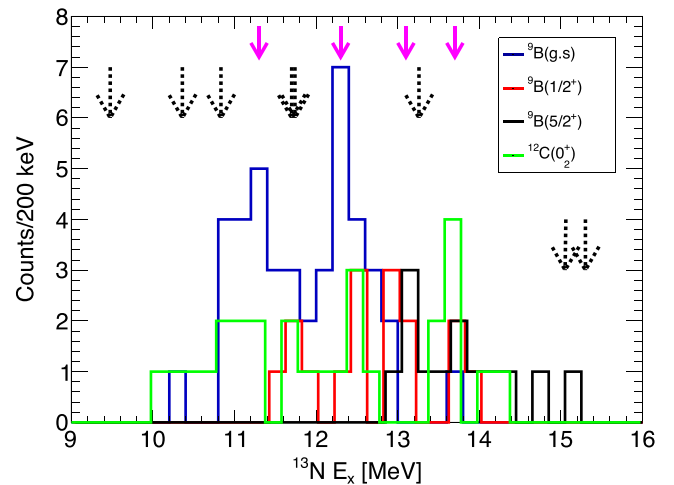


FIG. 5. Excitation spectrum in ${}^{13}\text{N}$ for $3\alpha + p$ separated by channels. Black dashed arrows show previously known states populated by β decay, and new states observed are shown by solid magenta arrows.

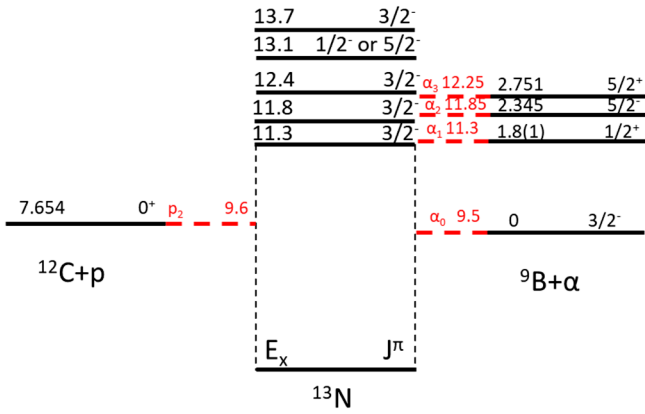


FIG. 6. Level scheme of measured $3\alpha + p$ states in ^{13}N in the central column with the proposed spin-parity assignments. The location of the thresholds for proton and α decay are shown in red with the equivalent excitation energy shown. The corresponding states in the daughter nuclei (^{12}C and ^9B) are also shown.

excitation energy of above 2.4 MeV. Any contribution from the relatively narrow 2.345 MeV $\frac{5}{2}^-$ (α_2) is not present in the presented plots, as this state decays almost exclusively via ^5Li and, therefore, would not correspond to a peak in the ^8Be spectrum. There were only three events associated with this decay to ^5Li ; hence, the statistics were insufficient to incorporate into the analysis.

Following the channel selection, the excitation energy in ^{13}N was calculated and is shown in Fig. 5. Despite low statistics, a number of states can be seen at 11.3, 12.4, 13.1, and 13.7 MeV. The location of these states relative to the thresholds for $^9\text{B} + \alpha$ and $^{12}\text{C}(0_2^+) + p$ is shown in Fig. 6. The clear peak structures [particularly apparent for the $\alpha + ^9\text{B}(\text{g.s.})$ channel] demonstrate the strength of this technique for studying cluster structures in ^{13}N . The nuclear structure implications of these states will be the topic of a follow-up paper that also includes more technical detail of the current work.

Conclusions.— β -delayed $3\alpha p$ decay has been observed for the first time. While β -delayed αp has been previously observed in ^9C [18], ^{17}Ne [19], ^{21}Mg [20], and ^{23}Si [21], these states did not provide any structural insight and instead were mainly seen through isobaric analog states that were well fed by β decay. In this Letter, $\beta 3\alpha p$ decay was observed from the states below the isobaric analog in ^{13}N at $E_x = 15$ MeV, demonstrating this is not merely a phase-space effect. The β -delayed $3\alpha p$ decays observed here are in strong competition with β -delayed proton decay, and, therefore, the states must have significant clustering. Evidence for the low-lying $\frac{1}{2}^+$ in ^9B in these background-free data, matching the parameters of previous observations [17], brings us closer to resolving the long-standing problem of searches for this elusive state. A paper will shortly be published that investigates the properties of the four new states observed here facilitated by this new technique and observed decay channel.

We thank Vlad Goldberg for helpful feedback on this work. This work was supported by the U.S. Department of Energy, Office of Science, Office of Nuclear Science under Grant No. DE-FG02-93ER40773 and by the National Nuclear Security Administration through the Center for Excellence in Nuclear Training and University Based Research (CENTAUR) under Grant No. DE-NA0003841. G. V. R. also acknowledges the support of the Nuclear Solutions Institute. S. A., S. M. C., C. H. K., D. K., S. H. K., and C. P. also acknowledge travel support from the IBS grant, funded by the Korean Government under Grant No. IBS-R031-D1. C. H. K. acknowledges travel support from the National Research Foundation of Korea (NRF) grant, funded by the Korea government (MSIT) (No. 2020R1A2C1005981 and No. 2013M7A1A1075764).

*jackbishop@tamu.edu

- [1] M. Pfützner, M. Karny, L. V. Grigorenko, and K. Riisager, *Rev. Mod. Phys.* **84**, 567 (2012).
- [2] B. Blank and M. Płoszajczak, *Rep. Prog. Phys.* **71**, 046301 (2008).
- [3] M. Seya, M. Kohno, and S. Nagata, *Prog. Theor. Phys.* **65**, 204 (1981).
- [4] W. von Oertzen, *Z. Phys. A* **354**, 37 (1996).
- [5] Y. Kanada-En'yo, M. Kimura, and A. Ono, *Prog. Theor. Exp. Phys.* **2012**, 01A202 (2012).
- [6] W. von Oertzen, H. G. Bohlen, M. Milin, T. Kokalova, S. Thummerer, A. Tumino, R. Kalpakchieva, T. N. Massey, Y. Eisermann, G. Graw, T. Faestermann, R. Hertenberger, and H.-F. Wirth, *Eur. Phys. J. A* **21**, 193 (2004).
- [7] M. Milin and W. von Oertzen, *Eur. Phys. J. A* **14**, 295 (2002).
- [8] H. Yamaguchi *et al.*, *Phys. Lett. B* **766**, 11 (2017).
- [9] M. Barbui, A. Volya, E. Aboud, S. Ahn, J. Bishop, V. Z. Goldberg, J. Hooker, C. H. Hunt, H. Jayatissa, T. Kokalova, E. Koshchiy, S. Pirrie, E. Pollacco, B. T. Roeder, A. Saastamoinen, S. Upadhyayula, C. Wheldon, and G. V. Rogachev, *Phys. Rev. C* **106**, 054310 (2022).
- [10] A. Volya, M. Barbui, V. Z. Goldberg, and G. V. Rogachev, *Commun. Phys.* **5**, 322 (2022).
- [11] H. H. Knudsen *et al.*, *Phys. Rev. C* **72**, 044312 (2005).
- [12] J. Bishop, G. V. Rogachev, S. Ahn, E. Aboud, M. Barbui, A. Bosh, C. Hunt, H. Jayatissa, E. Koshchiy, R. Malecek, S. T. Marley, E. C. Pollacco, C. D. Pruitt, B. T. Roeder, A. Saastamoinen, L. G. Sobotka, and S. Upadhyayula, *Phys. Rev. C* **102**, 041303(R) (2020).
- [13] J. Bishop *et al.*, *Nucl. Instrum. Methods Phys. Res., Sect. A* **964**, 163773 (2020).
- [14] R. Tribble, R. Burch, and C. Gagliardi, *Nucl. Instrum. Methods Phys. Res., Sect. A* **285**, 441 (1989).
- [15] E. Pollacco *et al.*, *Nucl. Instrum. Methods Phys. Res., Sect. A* **887**, 81 (2018).
- [16] J. Holmes, E. Galyaev, R. Alarcon, R. Acuna, D. Blyth, B. Fox, N. Mullins, and K. Scheuer, *J. Instrum.* **15**, T05001 (2020).

- [17] C. Wheldon, T. Kokalova, M. Freer, J. Walshe, R. Hertenberger, H.-F. Wirth, N.I. Ashwood, M. Barr, N. Curtis, T. Faestermann, R. Lutter, J.D. Malcolm, and D. J. Marín-Lámbbari, *Phys. Rev. C* **91**, 024308 (2015).
- [18] E. Gete, L. Buchmann, R.E. Azuma, D. Anthony, N. Bateman, J.C. Chow, J.M. D’Auria, M. Dombisky, U. Giesen, C. Iliadis, K.P. Jackson, J.D. King, D.F. Measday, and A.C. Morton, *Phys. Rev. C* **61**, 064310 (2000).
- [19] J.C. Chow, J.D. King, N.P.T. Bateman, R.N. Boyd, L. Buchmann, J.M. D’Auria, T. Davinson, M. Dombisky, E. Gete, U. Giesen, C. Iliadis, K. P. Jackson, A. C. Morton, J. Powell, and A. Shotter, *Phys. Rev. C* **66**, 064316 (2002).
- [20] M. Lund, M. Borge, J. Briz, J. Cederkäll, H. Fynbo, J. Jensen, B. Jonson, K. Laursen, T. Nilsson, A. Perea, V. Pesudo, K. Riisager, and O. Tengblad, *Phys. Lett. B* **750**, 356 (2015).
- [21] A. A. Ciemny *et al.*, *Phys. Rev. C* **106**, 014317 (2022).